p38-dependent c-Jun degradation contributes to reduced PGE$_2$ production in sodium orthovanadate-treated macrophages

Nur Aziz[1,#], Eunji Kim[1,#], Yanyan Yang[2,#], Han Gyung Kim[1], Tao Yu[3] & Jae Youl Cho[1,*]

[1]Department of Integrative Biotechnology and Biomedical Institute for Convergence at SKKU (BICS), Sungkyunkwan University, Suwon 16419, Korea, [2]Institute for Translational Medicine, School of Basic Medicine, Qingdao University, Qingdao, Shandong 266021, [3]Institute for Translational Medicine and Department of Cardiac Ultrasound, The Affiliated Hospital of Qingdao University, Qingdao, Shandong 266021, China

In particular, the phenomenon of c-Jun degradation within the inflammatory response has not yet been fully analyzed. In order to verify this, we investigated LPS-stimulated murine macrophages pre-treated with sodium orthovanadate (SO) in order to uncover the regulatory mechanisms of the MAPKs which regulate c-Jun degradation within the inflammatory response. Through our study, we found that SO suppressed the production of prostaglandin E$_2$ (PGE$_2$) and the expression of COX-2 in LPS-stimulated RAW264.7 cells. Additionally, SO decreased total c-Jun levels, without altering the amount of mRNA, although the phospho-levels of p38, ERK, and JNK were strongly enhanced. Through the usage of selective MAPK inhibitors, and knockdown and overexpression strategies, p38 was revealed to be a major MAPK which regulates c-Jun degradation. Further analysis indicates that the phosphorylation of p38 is a determinant for c-Jun degradation, and is sufficient to induce ubiquitination-dependent c-Jun degradation, recovered through MG132 treatment. Therefore, our results suggest that the hyperphosphorylation of p38 by SO contributes to c-Jun degradation, which is linked to the suppression of PGE$_2$ secretion in inflammatory responses; and thus, finding drugs to increase p38 activity could be a novel strategy for the development of anti-inflammatory drugs. [BMB Reports 2022; 55(8): 389-394]

INTRODUCTION

The activator protein-1 (AP-1) is a pivotal transcription factor that is responsible for the regulation of the transcription of various genes in response to inflammatory cytokines, stress inducers,

*Corresponding author. Tel: +82-31-290-7868; Fax: +82-31-290-7870; E-mail: jaecho@skku.edu
[#]These authors contributed equally to this work.

pathogens, and oncogenic stimuli (1). As such, AP-1 governs a variety of biological processes, including inflammation, proliferation, apoptosis, differentiation, survival, cell migration, and transformation (2). AP-1 contains Fos, Jun, and the activating transcription factor (ATF) protein dimers, all of which feature the evolutionarily-conserved basic region-leucine zipper (B-ZIP) DNA binding domain (1, 3). The composition of the dimers thereby also determines the sequence elements to which the AP-1 transcription factors bind to, and thus, may regulate specificity and subsequently execute certain distinct biological functions (4).

Jun, originally referred to as c-Jun, was first identified as a viral oncoprotein, and is one of the most characterized AP-1 subunits (5). There is long-standing evidence that c-Jun appears to be a major component of the AP-1 transcription factor complex, and that the identity of the c-Jun dimer partners determines the ability of the entire complex to transactivate AP-1-dependent transcription (6). It is well known that the AP-1 protein is a major target of and is primarily controlled by the mitogen-activated protein kinases (MAPKs), which both increase the abundance of AP-1 components and then directly stimulate their activity (6). Subfamilies of the MAPKs consist of extracellular signal-regulated protein kinases (ERK1 and ERK2), c-Jun N-terminal kinases (JNK1, JNK2, and JNK3), and p38s (p38α, p38β, p38γ, and p38δ), which are sequentially activated by MAPK kinases (MAPKKs) and their upstream MAPKK kinases (MAPKKKs) (7). During inflammatory responses, MAPK signaling is activated by phosphorylation, followed by the promotion of c-Jun transcriptional activity onto inflammatory cytokine genes. Growing evidence suggests that the c-Jun protein can also be regulated by other mechanisms, such as mRNA turnover and protein stability, thereby involving not only phosphorylation, but also cross-talking with other types of post-translational modifications, such as ubiquitination and sumoylation (2, 8).

c-Jun phosphorylation on its N-terminus is stabilizing, although the underlying mechanisms for c-Jun ubiquitination and degradation still remain largely undetermined, though recent findings have highlighted new players involved in the regulation of c-Jun degradation. For example, MEKK1 has been identified as mediating the ubiquitination of c-Jun in response to osmotic stress (8). Other ubiquitin ligases have also been reported to induce the

ubiquitination and degradation of c-Jun, such as COP1, Itch, and Fbw7 (9). Each player utilizes a similar, but different mechanism, depending on the c-Jun phosphorylation status. The overall regulation of c-Jun degradation is complex, as the phosphorylation status of c-Jun itself is a distinct process dictated by MAPKs depending on the cellular context; hence, the specific nature of the regulatory mechanism remains elusive.

Therefore, we deliver insights on a new player in c-Jun degradation regulation within the specific context of inflammatory responses. In efforts to elucidate the mechanism of c-Jun degradation, we utilize a phosphatase inhibitor, sodium orthovanadate (SO, Fig. 1A), and MAPK selective inhibitors within lipopolysaccharide (LPS)-stimulated murine macrophages.

RESULTS

SO treatment inhibits PGE$_2$ production and COX-2 expression in LPS-treated RAW264.7 cells

The inhibitory activity of SO was analyzed by determining the production level of PGE$_2$ amongst LPS-treated RAW264.7 cells in order to observe whether SO exhibited anti-inflammatory
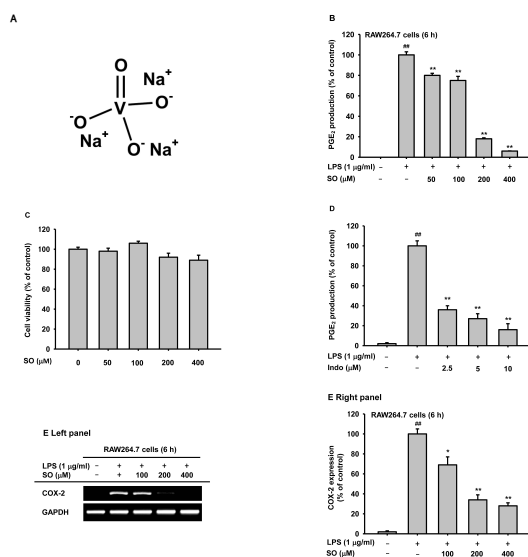
Fig. 1. SO treatment inhibits PGE$_2$ production and COX-2 expression among LPS-treated RAW264.7 cells. (A) The chemical structure of SO. (B, D) Inhibitory activity of SO or indomethacin on PGE$_2$ production was assessed among LPS-treated RAW264.7 cells (1 × 10^6 cells/ml) through the detection of PGE$_2$ release into the culture medium with an EIA kit. (C) The viability of SO-treated RAW264.7 cells (1 × 10^6 cells/ml) was determined through MTT assay. (E) The mRNA level of COX-2 among SO/LPS-treated RAW264.7 cells (1 × 10^6 cells/ml) was determined by semiquantitative (Left panel) and real-time (Right panel) PCR. Similar inhibitory patterns were observed in two repeat experiments. $^{##}P < 0.01$ compared to the normal group and $^*P < 0.05$ or $^{**}P < 0.01$ compared to control groups. Normal group: no-treatment group. Control group: LPS alone group.

activity. As shown in Fig. 1B, C, SO strongly diminished the release of PGE$_2$ at up to 95% at 400 μM, without altering cell viability. Indomethacin (Indo) also strongly downregulated PGE$_2$ production at 2.5, 5, and 10 μM. Simultaneously, the mRNA levels of COX-2 were measured by semiquantitative and real-time PCR to determine whether the inhibition of PGE$_2$ release by SO occurred at the gene expression level. As indicated by Fig. 1E, SO showed a remarkable ability to inhibit the mRNA expression of COX-2 at 200 and 400 μM.
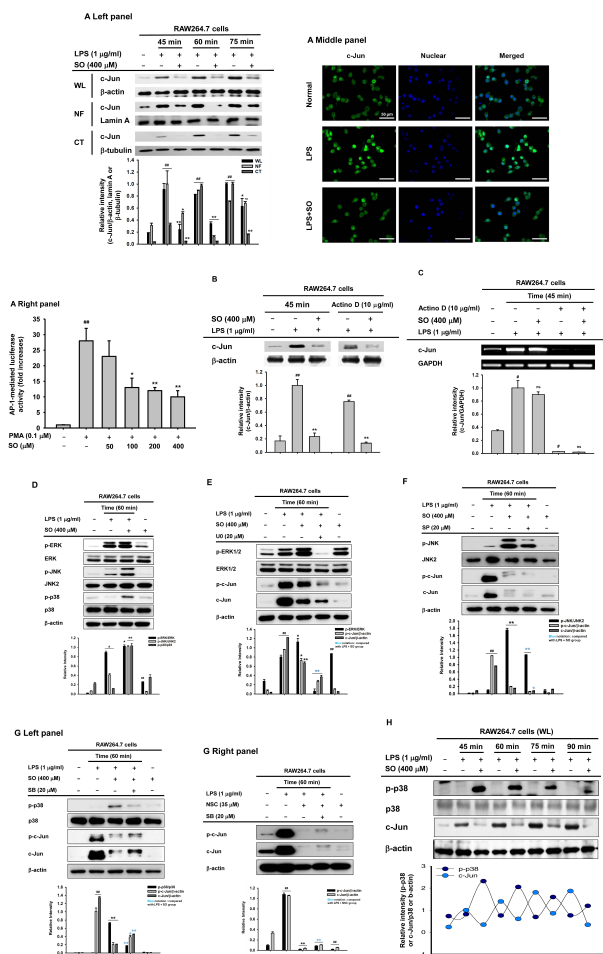
SO-mediated c-Jun depletion is not at the transcriptional level in LPS-stimulated RAW264.7 cells

In order to obtain a better understanding of the regulation of COX-2 expression by SO, we observed the level of c-Jun, as this transcription factor is a major subunit of AP-1, which plays a critical role in controlling COX-2 expression in RAW264.7 cells under LPS-stimulated conditions (10). An increased level of c-Jun was observed 45, 60, and 75 minutes after LPS treatment, while pre-treatment with SO showed a decrease in c-Jun levels, as caused by nuclear fractionation, immunofluorescence, and reporter gene assay (Fig. 2A). A decrease of c-Jun was observed in both the nuclear fraction and the cytosolic fraction (Fig. 2A, Left panel). Similar to these results, the nuclear levels of c-Jun were also remarkably decreased within the SO/LPS-treated group, when compared to LPS-stimulated cells (Fig. 2A, Middle panel). The luciferase activity increased by AP-1 was also dose-dependently inhibited through SO exposure (Fig. 2A, Right panel). Treatment with a transcription inhibitor, actinomycin D, revealed that the decreasing pattern of c-Jun protein abundance through SO-treatment could still be observed (Fig. 2B). Additionally, c-Jun mRNA expression appeared to be similar after SO pre-treatment among LPS-stimulated RAW264.7 cells, both with and without Actino D treatment (Fig. 2C), indicating that SO did not inhibit the transcriptional process of c-Jun. Immunoblotting analysis of these proteins was then carried out to examine whether SO could also affect the phosphorylation level of MAPKs and upstream enzymes in order to control c-Jun activation. As depicted by Fig. 2D, SO increased the levels of p-p38, p-ERK, and p-JNK at 45 minutes after LPS treatment.

SO-mediated c-Jun degradation is mediated by p38 in LPS-stimulated RAW264.7 cells

Under LPS stimulation, MAPKs such as p38, ERK, and JNK, are phosphorylated and subsequently induce the activation of c-Jun through phosphorylation. Previous studies have indicated that the phosphorylation of c-Jun plays a role in governing the stability of c-Jun protein levels. To confirm which upstream enzymes dominate the regulation of this process, we utilized MAPK-specific inhibitors among SO/LPS-treated RAW264.7 cells. The co-treatment with U0126 (U0) or SP600125 (SP), and the selective inhibitors of ERK and JNK, respectively, were still able to further promote SO-mediated c-Jun degradation (Fig. 2E, F). Contrary to expectations, co-treatment with SB203580 (SB), a selective inhibitor of p38, showed no further decreasing of

Fig. 2. SO-mediated c-Jun depletion does not occur at the transcriptional level among LPS-stimulated RAW264.7 cells. (A, Left panel; B, D-H) RAW264.7 cells (1 × 10^6 cells/ml) were pre-treated with SO (400 μM) for 30 minutes, followed by LPS (1 μg/ml) incubation for the indicated times, both in the absence or presence of actinomycin D (Actino D), U0, SP, SB, or NSC. The levels of c-Jun, p-c-Jun, p-ERK, ERK, p-p38, p38, p-JNK, JNK, and β-actin from cellular factions [nuclear fraction (NF) and cytosolic fraction (CF)] or whole-cell lysates (WL) were detected through immunoblotting analysis. (A, Middle panel) The immunofluorescence of c-Jun after pre-treatment with SO among LPS-stimulated RAW264.7 cells was observed through confocal microscopy. (A, Right panel) RAW264.7 cells were transfected with AP-1-Luc, as well as β-gal (as a transfection control) plasmid constructs, and were treated with SO in the presence or absence of PMA (100 nM) for 12 hours. Luciferase activity was determined through luminometry. (C) c-Jun mRNA expression was determined through semiquantitative reverse transcriptase (RT)-PCR analysis after pre-treatment, with or without Actino D/SO among LPS-stimulated RAW264.7 cells. #P < 0.05 or ##P < 0.01 compared to the normal group and *P < 0.05 or **P < 0.01 compared to control groups. Normal group: no-treatment group. Control group: LPS or PMA alone group. Blue notation: compared to LPS + SO or NSC group.

c-Jun protein levels following SO treatment among LPS-stimulated RAW264.7 cells (Fig. 2G, Left panel). Interestingly, this phenomenon also occurred following the usage of another phosphatase inhibitor, NSC95397 (NSC: 2,3-bis-[(2-hydroxyethyl)thio]-1,4-naphthoquinone), and further decreases in c-Jun levels were not shown after co-treatment with SB (Fig. 2G, Right panel). Moreover, the phosphorylation pattern of p38 and the decreased level of c-Jun were also detected through immunoblotting analysis. The phosphorylation level of c-Jun at Ser73 also exhibited a similar level, as the c-Jun total formed under all conditions after treatment with U0, SP, and SB, indicating that the direct correlation between the phosphorylation of c-Jun and the c-Jun total form level. These results thereby suggest that p38 plays a dominant role in regulating c-Jun degradation amongst LPS-stimulated macrophages. The activation of p38 by SO was also examined amongst LPS-treated RAW264.7 cells. As shown by Fig. 2H, interestingly, SO strongly enhanced the level of p-p38 from 45 to 90 minutes during LPS exposure, whereas LPS alone upregulated the c-Jun levels at these time markers.

p38 positively regulates c-Jun degradation

To confirm the dependency of c-Jun degradation on p38, we performed knockdown and over-expression experiments. Initially, we performed a knockdown of p38 with siRNA, and confirmed the knockdown efficiency (up to a 70% decrease) through real-time PCR (Fig. 3A, Left panel). The knockdown of p38 indicated that no change was observed amongst c-Jun protein levels in LPS-stimulated RAW264.7 cells (Fig. 3A, Middle panel). Treatment with p38 siRNA with an increasing concentration gave clear indication of the recovery of c-Jun protein levels following SO-mediated c-Jun degradation among RAW264.7 cells (Fig. 3A, Right panel). These data exhibited consistent results when compared to the immunoblotting results using a p38-selective inhibitor. Moreover, the overexpression of p38 was sufficient to induce c-Jun degradation among RAW264.7 cells (Fig. 3B). These results indicated that p38 positively regulates c-Jun degradation. As the ectopic expression of p38 results in a decrease of RAW264.7 cell c-Jun protein levels, while both knockdown and p38-selective inhibition showed c-Jun recovery, we hypothesized that the phosphorylation of p38 is a driving force for c-Jun degradation among RAW264.7 cells. Additionally, the co-transfection of p38 and c-Jun among HEK293T cells following SO treatment revealed that SO inhibited the binding between p38 and c-Jun through immunoprecipitation assay (Fig. 3C). *In-vitro* kinase assay using immunoprecipitated p-p38 and c-Jun as substrate sources indicated that p-p38 directly induced the phosphorylation of c-Jun (Fig. 3D), thus implying that c-Jun degradation may require p38-mediated phosphorylation of c-Jun at Ser73.

To further analyze to what extent the phosphorylation of p38 regulates c-Jun degradation, we extended the line of inquiry from our previous hypothesis, to suggest that the phosphorylation of p38 plays an important role in c-Jun degradation. The co-transfection of p38 and adaptor protein TRIF showed a strong
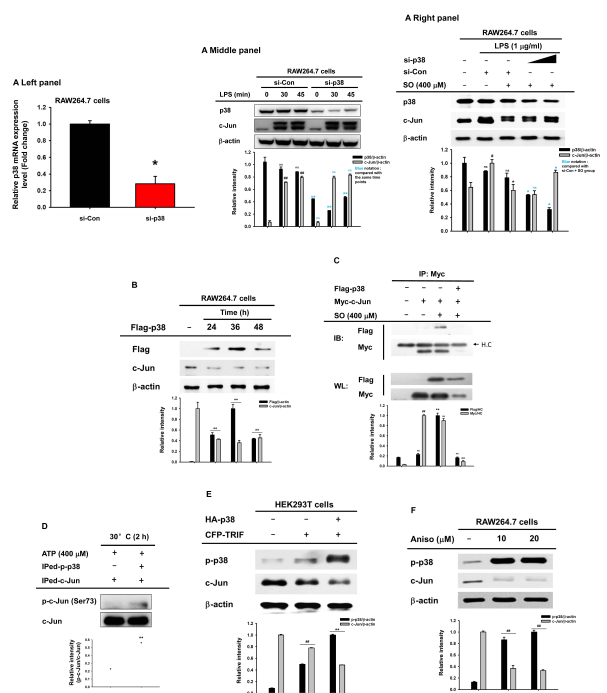
Fig. 3. p38 positively regulates c-Jun degradation. (A, Left panel) RAW264.7 cells were transfected with siRNA against p38. The knockdown level of p38 was measured through real-time PCR. (A, Middle panel) Two days after transfection, the cells were treated with LPS (1 μg/ml) for the indicated times. Immunoblotting analysis was performed in order to detect the levels of p38 and c-Jun among RAW264.7 cells with p38-knockdown after LPS stimulation. (A, Right panel) Immunoblotting analysis was carried out in order to detect the levels of p38 and c-Jun among RAW264.7 cells with p38-knockdown during either SO or LPS exposure. (B) RAW264.7 cells were transfected with Flag-p38 for the indicated times, and then Flag and c-Jun levels were analyzed through immunoblotting analysis. (C) HEK293T cells were transfected with Flag-p38 and Myc-c-Jun for 24 hours, followed by SO treatment. After preparing cell lysates, immunoprecipitation and immunoblotting analyses were performed in order to check the levels of Flag and Myc. (D) IP-kinase assay was then performed in the presence or absence of enzyme (immunoprecipitated p-p38) and substrate (immunoprecipitated c-Jun). Immunoblotting analysis was then performed to determine the levels of phospho-c-Jun and c-Jun. (E) HEK293T (2×10^6 cells/ml) cells were then transfected with HA-p38 and CFP-TRIF for 24 hours. The levels of p-p38 and c-Jun were detected through immunoblotting analysis. (F) RAW264.7 cells were treated with Anisomycin (Aniso) for 24 hours at the indicated concentrations. The levels of p-p38 and c-Jun were detected through immunoblotting analysis. [#]$P < 0.05$ or [##]$P < 0.01$ compared to the normal group and *$P < 0.05$ or **$P < 0.01$ compared to control groups. Normal group: (A Middle panel) si-Con without LPS (0 min), (A Right panel) without LPS treatment, (C) Flag-p38 (−) + Myc-c-Jun (−) + SO (−), (E) HA-p38 (−) + CFP-TRIF (−), (F) Aniso (−). Control group: (A Left panel) si-Con, (A Right panel) si-Con + LPS, (B) Flag-p38 (−), (C) Myc-c-Jun (+), (D) ATP (+) + IPed-c-Jun (+), IPed-p-p38 (−), (E) CFP-TRIF (+). Blue notation: (A Middle panel) compared to the same time points, (A Right panel) compared with si-Con + SO (+).

increase in the phosphorylation of p38 while, as expected, a decreased level of c-Jun was observed (Fig. 3E). Additionally, we treated RAW264.7 cells with anisomycin, a well-characterized p38 activator and protein synthesis inhibitor. The anisomycin treatment increased the phosphorylation of p38, and also induced c-Jun degradation among RAW264.7 cells (Fig. 3F).

p38-mediated c-Jun degradation is ubiquitin-dependent
Ubiquitination-dependent c-Jun degradation has been widely analyzed (11), but whether SO-induced c-Jun degradation is ubiquitin-proteasome dependent still remains unknown. In this study, we utilized MG132, a known proteasome inhibitor, in order to identify the ubiquitin-proteasome dependencies within SO-mediated c-Jun degradation among LPS-stimulated RAW264.7 cells. Pre-treatment with MG132 led to a clear recovery of c-Jun protein levels following SO-mediated c-Jun degradation among LPS-stimulated RAW264.7 cells (Fig. 4A), which indicated that SO-mediated c-Jun degradation is a ubiquitin-proteasome-dependent event. We confirmed this regulation by inducing the overexpression of p38 and TRIF among HEK293T cells with the addition of MG132. As indicated by Fig. 4B, c-Jun protein levels were consistently recovered within the MG132-treated group, and using a similar design, we performed c-Jun immunoprecipitation and immunoblotting analysis with the usage of ubiquitin antibodies. Interestingly, increased band intensity was detected in the blot with a molecular weight around 43−48 kDa, within which c-Jun was present (Fig. 4C).

DISCUSSION

In order to expand the regulatory mechanisms of MAPK signaling with respect to c-Jun degradation, we used SO, a tyrosine phosphatase inhibitor, which has been reported to induce MAPK activation (12). LPS treatment increased both c-Jun mRNA and protein levels (Fig. 2A, C), and intriguingly, the treatment with SO reduced the c-Jun protein level, but not its mRNA level, among LPS-induced murine macrophages (Fig. 2A, C). This decrease in c-Jun protein levels could be due to a decrease in transcription or post-translational modification through proteasome degradation. According to our results, SO was found to regulate c-Jun degradation, but not at the transcriptional level. This supports the plausible implication that tyrosine phosphorylation induced the MAPK signaling during the regulation of c-Jun degradation. In addition, we observed that only the selective p38 inhibitor was able to recover the c-Jun protein levels following SO-mediated depletion, whereas JNK and ERK inhibitors failed to do so (Fig. 3). Interestingly, NSC95397, an irreversible Cdc25 dual specificity phosphatase inhibitor, was shown to also induce a decrease in c-Jun protein levels, and further decreases were not observed after treatment with p38-selective inhibitor (Fig. 2G, Right panel). The results also showed that SO strongly induced the phosphorylation of p38, while c-Jun levels were also decreased by this compound among LPS-treated RAW264.7 cells (Fig. 2H). Interestingly, the levels
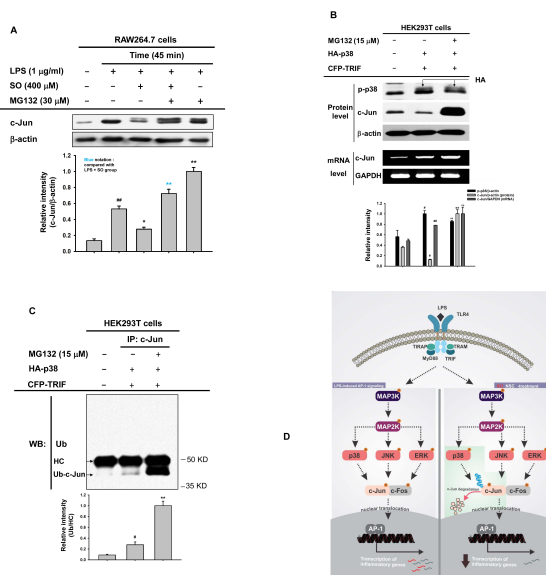
Fig. 4. p38-mediated c-Jun degradation is ubiquitin-dependent. (A) RAW264.7 cells (1×10^6 cells/ml) were pre-treated with SO (400 µM), followed by LPS (1 µg/ml) incubation for 45 minutes, and then further treated with MG132 (30 µM) 4 hours before harvesting the cells. The levels of c-Jun were analyzed by immunoblotting analysis. (B) HEK293T cells were transfected with HA-p38 and CFP-TRIF for 24 hours. MG132 (15 µM) was then added 4 hours prior to cell harvesting. The protein levels of p-p38, c-Jun, and β-actin and mRNA levels of c-Jun and GADPH were then analyzed through immunoblotting and RT-PCR. (C) HEK293T cells were transfected with HA-p38 and CFP-TRIF for 24 hours. MG132 (15 µM) was then added 4 hours prior to cell harvesting. Cell lysates were then subjected to immunoprecipitation with c-Jun antibodies, and the levels of Ub were detected through immunoblotting analysis. (D) A schematic illustration depicting the dominant role of p38 in the regulation of c-Jun degradation. $^{\#}P < 0.05$ or $^{\#\#}P < 0.01$ compared to the normal group and $*P < 0.05$ or $**P < 0.01$ compared to control groups. Normal group: (A) without treatment, (B; C) MG132 (−) + HA-p38 (−) + CFP-TRIF (−). Control group: (A) LPS alone, (B; C) HA-p38 (+) + CFP-TRIF (+).

of p-p38 (seen between 0 to 30 min) and c-Jun (seen between 45 to 120 min) showed opposite patterns in LPS-treated RAW264.7 cells (data not shown). These results further demonstrated that p38 is a major MAPK within the regulation of c-Jun degradation under SO-treated conditions.

The knockdown and overexpression of p38 confirmed the positive regulation by p38 on c-Jun degradation. Similar to JNK, p38 has been demonstrated to directly phosphorylate c-Jun at Ser-63 and Ser-73, and thus modulate the transcriptional activity of AP-1 (13). Based on our data, the phosphorylation of p38 appears to play an important and sufficient role in inducing c-Jun ubiquitination (Fig. 4). However, the dependencies of c-Jun degradation, with respect to the particular site of c-Jun phosphorylation, still remain elusive. GSK3 phosphorylates c-Jun at Ser243 and Thr239, which are required for Fbw7-mediated c-Jun degradation (14). C-terminal Src kinase has been shown

to bind with, and directly phosphorylate, c-Jun at Y26 and Y170, promoting c-Jun degradation and reduced stability (15). Of particular note, our findings indicate that there is a major involvement of p38 in c-Jun degradation during inflammatory response conditions. However, whether p38 can directly phosphorylate c-Jun at similar phosphorylation sites, and subsequently mediate c-Jun degradation, is a question that must be addressed in future studies. In addition, because phosphorylation of p38 is governed by both upstream kinases and particular phosphatases, it is also important to identify the exact molecular player, if it happens that p38 is not the direct regulator of this mechanism. Our results shed light on a plausible, novel p38/c-Jun molecular axis which governs c-Jun degradation during the inflammatory response.

Conclusively, we found that phosphatase inhibition governing MAPK signaling mediates c-Jun degradation among LPS-stimulated RAW264.7 cells. Additionally, further analysis indicated that the dominant role of p38 in the positive regulation of c-Jun degradation in an inflammatory response model, as summarized in Fig. 4D. The phosphorylation of p38 promotes c-Jun degradation through the induction of c-Jun protein ubiquitination. These results highlighted the novel regulatory role of p38 within the inflammatory response through the regulation of the protein level of c-Jun/AP-1 transcription factors.

MATERIALS AND METHODS

Materials
Sodium orthovanadate was purchased from Sigma-Aldrich (St. Louis, MO, USA). Phosphospecific or total-protein antibodies were purchased from Cell Signaling Technology (Beverly, MA, USA).

Cell culture
RAW264.7 cells (ATCC number TIB-71) and HEK293T cells (ATCC number CRL-1573) were cultured in RPMI 1640 and DMEM media, respectively.

Determination of PGE$_2$ level
The inhibitory effect of SO on the production of PGE$_2$ was determined by analyzing the level of PGE$_2$ using EIA kits, as previously described (16).

Cell viability test
The viability of SO-treated RAW264.7 cells was checked by a conventional MTT assay, as previously reported (17).

Preparation of whole-cell lysates, nuclear fractions, and immunoblotting analysis
Preparation of whole-cell lysates was done as described previously (18). Nuclear fractionation was done according to a previous report (18). Immunoblotting analysis of both nuclear fractionation and whole-cell lysates was performed as indicated previously (18).

Immunofluorescence-Confocal microscopy

After washing the cells, Confocal microscopic analysis was carried out according to previous reports (19).

Plasmid DNA and siRNA transfection

See Supplementary data section.

mRNA expression analysis by semiquantitative reverse transcriptase (RT)-polymerase chain reaction (PCR) and real-time PCR

Analysis of mRNA expression by semiquantitative RT-PCR and real-time PCR was performed as previously described (20). The primer sequences were used as reported previously (21, 22).

Immunoprecipitation (IP)

Immunoblotting analyses were then performed using these lysates prepared with immunoprecipitation buffer previously reported (21).

IP-kinase assay

See Supplementary data section.

Statistical analysis

See Supplementary data section.

ACKNOWLEDGEMENTS

CONFLICTS OF INTEREST

The authors have no conflicting interests.

REFERENCES

1. Hess J, Angel P and Schorpp-Kistner M (2004) AP-1 subunits: quarrel and harmony among siblings. J Cell Sci 117, 5965-5973
2. Ye N, Ding Y, Wild C, Shen Q and Zhou J (2014) Small molecule inhibitors targeting activator protein 1 (AP-1). J Med Chem 57, 6930-6948
3. Han SW, Jung BK and Ryu KY (2021) Regulation of polyubiquitin genes to meet cellular ubiquitin requirement. BMB Rep 54, 189-195
4. Tran TT, Song WH, Lee G et al (2021) Avenanthramide C as a novel candidate to alleviate osteoarthritic pathogenesis. BMB Rep 54, 528-533
5. Eferl R and Wagner EF (2003) AP-1: a double-edged sword in tumorigenesis. Nat Rev Cancer 3, 859-868
6. Whitmarsh AJ (2007) Regulation of gene transcription by mitogen-activated protein kinase signaling pathways. Biochim Biophys Acta 1773, 1285-1298
7. Turjanski AG, Vaqué JP and Gutkind JS (2007) MAP kinases and the control of nuclear events. Oncogene 26, 3240-3253
8. Xia Y, Wang J, Xu S et al (2007) MEKK1 mediates the ubiquitination and degradation of c-Jun in response to osmotic stress. Mol Cell Biol 27, 510-517
9. Welcker M and Clurman BE (2008) FBW7 ubiquitin ligase: a tumour suppressor at the crossroads of cell division, growth and differentiation. Nat Rev Cancer 8, 83-93
10. Zhang J, Kim MY and Cho JY (2020) Euodia pasteuriana methanol extract exerts anti-inflammatory effects by targeting TAK1 in the AP-1 signaling pathway. Molecules 25, 5760
11. Park GH, Park JH and Chung KC (2021) Precise control of mitophagy through ubiquitin proteasome system and deubiquitin proteases and their dysfunction in Parkinson's disease. BMB Rep 54, 592-600
12. Jayakumar C, Mohamed R, Ranganathan PV and Ramesh G (2011) Intracellular kinases mediate increased translation and secretion of netrin-1 from renal tubular epithelial cells. PLoS One 6, e26776-e26776
13. Humar M, Loop T, Schmidt R et al (2007) The mitogen-activated protein kinase p38 regulates activator protein 1 by direct phosphorylation of c-Jun. Int J Biochem Cell Biol 39, 2278-2288
14. Wei W, Jin J, Schlisio S, Harper JW and Kaelin WG Jr (2005) The v-Jun point mutation allows c-Jun to escape GSK3-dependent recognition and destruction by the Fbw7 ubiquitin ligase. Cancer Cell 8, 25-33
15. Zhu F, Choi BY, Ma W-Y et al (2006) COOH-terminal Src kinase-mediated c-Jun phosphorylation promotes c-Jun degradation and inhibits cell transformation. Cancer Res 66, 5729-5736
16. Cho JY, Baik KU, Jung JH and Park MH (2000) In vitro anti-inflammatory effects of cynaropicrin, a sesquiterpene lactone, from Saussurea lappa. Eur J Pharmacol 398, 399-407
17. Yayeh T, Jung KH, Jeong HY et al (2012) Korean Red Ginseng saponin fraction downregulates proinflammatory mediators in LPS stimulated RAW264.7 cells and protects mice against endotoxic shock. J Ginseng Res 36, 263-269
18. Aziz N, Kang Y-G, Kim Y-J et al (2020) Regulation of 8-hydroxydaidzein in IRF3-mediated gene expression in LPS-stimulated murine macrophages. Biomolecules 10, 238
19. Jeong D, Lee J, Park SH et al (2019) Antiphotoaging and antimelanogenic effects of penthorum chinese pursh ethanol extract due to antioxidant- and autophagy-inducing properties. Oxid Med Cell Longev 2019, 9679731
20. Aziz N, Son YJ and Cho JY (2018) Thymoquinone suppresses IRF-3-mediated expression of type i interferons via suppression of TBK1. Int J Mol Sci 19, 1355
21. Yang WS, Kim HG, Lee Y et al (2020) Isoprenylcysteine carboxyl methyltransferase inhibitors exerts anti-inflammatory activity. Biochem Pharmacol 182, 114219
22. Lee JO, Kim JH, Kim S et al (2020) Gastroprotective effects of the nonsaponin fraction of Korean Red Ginseng through cyclooxygenase-1 upregulation. J Ginseng Res 44, 655-663